

Matrix Isolation and *ab Initio* Study of the Hydrogen-Bonded Complex between H₂O₂ and (CH₃)₂O

James Goebel and Bruce S. Ault*

Department of Chemistry, University of Cincinnati, P.O. Box 210172, Cincinnati, Ohio 45221-0172

Janet E. Del Bene

Department of Chemistry, Youngstown State University, Youngstown, Ohio 44555

Received: November 23, 1999; In Final Form: January 4, 2000

Matrix isolation infrared spectroscopy has been combined with MP2/6-31+G(d,p) calculations to characterize the 1:1 hydrogen-bonded complex between H₂O₂ and (CH₃)₂O. The O–H stretching mode was observed to red shift 234 cm⁻¹ upon hydrogen bond formation, while a 45 cm⁻¹ blue shift was noted for the O–O–H bending mode of the H₂O₂ subunit in the complex. These values compare well to the computed shifts of -293 and +20 cm⁻¹, respectively. The perturbations to the vibrational modes of the two subunits in the HOOH:O(CH₃)₂ complex are substantially larger than the perturbations reported previously for the analogous HOH:O(CH₃)₂ complex, suggesting that H₂O₂ is a better proton donor for hydrogen bonding than H₂O. In contrast, band shifts in HOOH:O(CH₃)₂ are much less than observed for FH:O(CH₃)₂ and ClH:O(CH₃)₂.

Introduction

Hydrogen peroxide is a molecule of interest in a large and diverse number of fields, including atmospheric chemistry and biochemistry.^{1–3} Although some research has been done, the role of hydrogen bonding in the chemistry of hydrogen peroxide is not well understood.^{4–6} Gas phase, solvent-free studies of H₂O₂ are technically difficult, and solution-phase studies are complicated by the role of the solvent. On the other hand, theoretical studies of the chemistry of H₂O₂ have sought to explore intermediates and transition states, as well as the role of small numbers of solvent molecules.^{5,6}

The matrix isolation technique was developed for the isolation, stabilization, and spectroscopic characterization of reactive or short-lived species in inert cryogenic matrixes.^{7,8} Species that have been studied in this manner include radicals, ions, and weakly bound molecular complexes. While matrix isolation would seem to be ideal for the study of the chemistry of hydrogen peroxide, relatively little work has been done because of the problems and dangers associated with handling pure hydrogen peroxide.^{9–11} Recently, Rasanen and co-workers demonstrated that the urea–hydrogen peroxide adduct is a safe source of solvent-free gas-phase hydrogen peroxide, which may then be used in matrix isolation experiments.¹² As a result of the high interest in the chemistry of H₂O₂, a series of studies has been initiated to examine the ability of H₂O₂ to participate in hydrogen bonding interactions. Dimethyl ether, (CH₃)₂O, was selected as the reaction partner because it has been extensively studied with other hydrogen bond donors, including water and hydrogen halides.^{13–15} *Ab initio* calculations have also been carried out to provide structural and energetic data for HOOH:O(CH₃)₂ and to assist in the interpretation of the experimental spectra.

Experimental Section

The experiments in this study were carried out on matrix isolation equipment that has been described elsewhere,¹⁷ with

modification for the generation and deposition of H₂O₂. To generate H₂O₂, the urea–hydrogen peroxide adduct (UHP) was obtained from Acros in the form of 1 g tablets. A tablet was coarsely ground with a mortar and pestle under a nitrogen atmosphere and the fines (smaller than 20 mesh) were discarded. The remaining sample (~0.5 g) was placed in the bottom of a U-shaped tube made of 1/4 in. Teflon-FEP tubing. The U-tube was connected to the manifold on one side and 1/8 in. FEP tubing on the other side. This 1/8 in. tubing was directly attached to the cryostat chamber. Preparation of d₂-UHP was carried out by dissolving 0.5 g of UHP in 2 mL of D₂O at 60 °C.¹⁶ Using relative band intensities for H₂O₂, HDO₂, and D₂O₂ and the fact that an O–D oscillator has about half the intensity of a comparable O–H oscillator, the D/H ratio in the D₂O₂ samples is estimated to be 3/1. Upon cooling, the deuterated UHP crystallized and the remaining water was removed under vacuum. Between experiments the UHP was kept at 0 °C, and during experiments a circulator bath was used to maintain the UHP at a constant temperature. The temperature range employed for H₂O₂ vaporization in these experiments was 2–15 °C. (CH₃)₂O (Matheson) and (CD₃)₂O (MSD Isotopes) were introduced into the vacuum line as gases and purified by repeated freeze–pump–thaw cycles at 77 K. Argon was the matrix gas in all experiments and was used without further purification.

Most experiments were conducted in the twin jet mode in which the Ar/H₂O₂ and Ar/(CH₃)₂O samples were deposited from separate nozzles on the cryogenic surface at 14 K. One experiment was conducted using merged jet deposition in which the stainless steel line from the (CH₃)₂O manifold was connected to the FEP tubing from the H₂O₂ manifold with a Teflon tee. A 1/8 in. FEP tube approximately 30 cm long connected the tee to the cryostat chamber. Samples were deposited for 20–24 h at an approximate flow rate of 2 mmol/h from each manifold. Spectra were recorded on a Mattson Cygnus FTIR at 1 cm⁻¹ resolution. A total of 250 scans were averaged for both background and sample spectra. Some matrixes were then

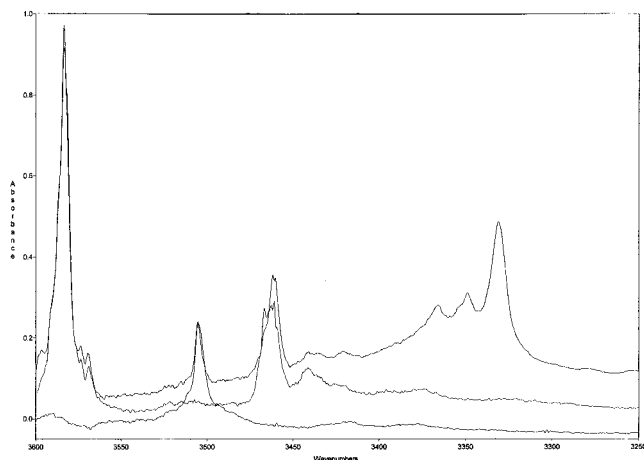


Figure 1. Upper trace: Ar:H₂O₂ co-deposited with Ar:(CH₃)₂O = 1000:1. Middle trace: Ar:H₂O₂ co-deposited with Ar. Lower trace: Ar co-deposited with Ar:(CH₃)₂O = 1000:1. The band appearing in the upper and lower traces near 3505 cm⁻¹ is due to the HOH:O(CH₃)₂ complex, while the band appearing near 3455 cm⁻¹ in the middle and upper traces is due to (H₂O)₂.

annealed to as high as 36 K, recooled to 14 K, and additional spectra were recorded.

Method of Calculation

Ab initio calculations at second-order Moller–Plesset perturbation theory [MBPT(2) = MP2]^{18–21} have been carried out with the 6-31+G(d,p) basis set^{22–25} to determine the optimized structures of hydrogen peroxide (H₂O₂), dimethyl ether [(CH₃)₂O], and the hydrogen-bonded complex HOOH:O(CH₃)₂. The MP2/6-31+G(d,p) level of theory provides structures and binding energies of hydrogen-bonded complexes that are in reasonable agreement with experimental data and is the minimum level of theory required to obtain frequency shifts of the hydrogen-bonded X–H stretching band in an X–H–Y hydrogen bond provided that anharmonic effects are not unusually large.^{26–29} Harmonic vibrational frequencies were computed to establish that all structures are equilibrium structures on their respective potential energy surfaces, to obtain zero-point vibrational energies, and to simulate the vibrational spectrum of the complex. All calculations were carried out using the Gaussian 94 suite of programs³⁰ on the Cray T94 supercomputer at the Ohio Supercomputer Center.

Experimental Results

Before co-deposition experiments were run, blank spectra of H₂O₂ and (CH₃)₂O in solid argon were obtained in separate experiments. These spectra agree with published data and spectra previously obtained in this laboratory.³¹ While some (H₂O)₂ was present in all experiments and was in greater abundance in experiments run at higher concentrations, the monomer was the dominant species present in all H₂O₂ blank and co-deposition experiments.

H₂O₂ + (CH₃)₂O. In an initial experiment argon swept over UHP at 8 °C was co-deposited with (CH₃)₂O in Ar in the ratio Ar:O(CH₃)₂ of 250:1. Several distinct product bands were noted, the most prominent of which was a broad feature centered around 3349 cm⁻¹, with three partially resolved maxima at 3367, 3349, and 3332 cm⁻¹, as shown in Figure 1. Two weak product bands were observed at 1315 and 672 cm⁻¹; this latter band is shown in Figure 2. In addition, several of the bands attributable

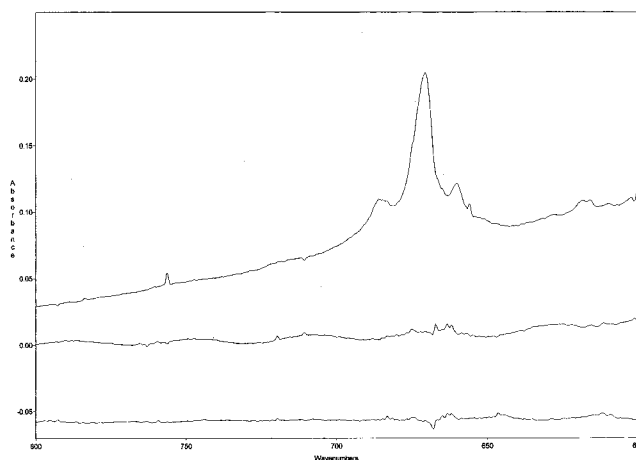


Figure 2. Upper trace: Ar:H₂O₂ co-deposited with Ar:(CH₃)₂O = 500:1. Middle trace: Ar:H₂O₂ co-deposited with Ar. Lower trace: Ar co-deposited with Ar:(CH₃)₂O = 1000:1.

to (CH₃)₂O were broadened or had unresolved shoulders when compared to the spectrum of pure (CH₃)₂O.

A total of 10 experiments were then conducted in which the temperature of the UHP (and thus the concentration of H₂O₂) was varied from 2 to 15 °C and the Ar:(CH₃)₂O concentration varied from 100:1 to 1000:1. In all of these experiments, the bands at 3367, 3349, 3332, 1315, and 672 cm⁻¹ were present with intensities that varied directly with the concentrations of the reactants. In the experiments conducted at low (CH₃)₂O concentrations, several of the previously unresolved shoulders on the parent absorptions were sufficiently well resolved to measure band positions. These product bands were located at 2943, 2829, 1165, 1090, and 914 cm⁻¹. The one merged jet experiment showed no significant differences from the twin jet experiments.

H₂O₂ + (CD₃)₂O. Four experiments were conducted in which the temperature of the UHP (and thus the concentration of H₂O₂) was varied from 2 to 11 °C and the Ar:(CD₃)₂O concentration varied from 500:1 to 1000:1. In all the experiments the same broad feature noted above with three partially resolved maxima was present. These maxima were at 3365, 3346, and 3329 cm⁻¹. The bands at 1315 and 672 cm⁻¹ were also still present. Several product bands near parent modes of (CD₃)₂O were sufficiently well resolved that band positions could be determined. These bands were at 2249, 2207, 2065, 1136, and 817 cm⁻¹. In one of these experiments (UHP at 8 °C: Ar:(CD₃)₂O, 500:1), the matrix was annealed to 36 K and after cooling back below 20 K another spectrum was taken. All of the product bands grew in roughly the same proportions with no new product bands appearing.

D₂O₂ + (CH₃)₂O. One experiment was performed in which a sample of Ar/D₂O₂ was co-deposited with a sample of Ar:(CH₃)₂O = 250:1. In addition to the bands from each reactant several product bands were observed. A broad feature consisting of four partially resolved bands was centered at 2481 cm⁻¹. The individual maxima were located at 2493, 2483, 2479, and 2468 cm⁻¹ with the band at 2468 cm⁻¹ being the most intense, as shown in Figure 3. Two weak bands were observed at 1090 and 913 cm⁻¹ while one very weak band was observed at 501 cm⁻¹. In this experiment the matrix was also annealed to 36 K and recooled to 14 K and an additional spectrum recorded. All of the above product bands increased in intensity, while no new product bands appeared. Table 1 lists all of the band positions observed in all of the experiments conducted in this study.

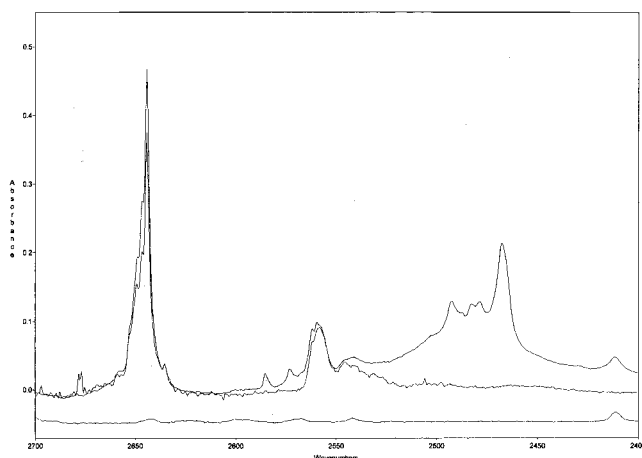


Figure 3. Upper trace: Ar:D₂O₂ co-deposited with Ar:(CH₃)₂O = 500:1. Middle trace: Ar:D₂O₂ co-deposited with Ar:(CH₃)₂O = 1000:1. Lower trace: Ar co-deposited with Ar:(CH₃)₂O = 1000:1.

TABLE 1: Experimental Frequencies for Vibrational Bands in the Hydrogen Peroxide and Dimethyl Ether Monomers and Complexes

H ₂ O ₂	(CH ₃) ₂ O	(CD ₃) ₂ O	D ₂ O ₂	HOOH: O(CH ₃) ₂	HOOH: O(CD ₃) ₂	DOOD: O(CH ₃) ₂
3583				3367	3365	
				3349	3346	
				3332	3329	
	2986			2997		
	2922			2943		
	2889			2897		
	2820			2826		
			2644			2493
						2483
						2479
						2468
		2190			2207	
		2061			2065	
		2056			2061	
1270		1315			1315	
	1168			1165		
	1098			1090		1090
	925			914		913
		823			817	
				672	672	
						501

Results of *ab Initio* Calculations

Only one equilibrium structure was found for HOOH:O(CH₃)₂ on the MP2/6-31+G(d,p) potential surface. The equilibrium structure has C₁ symmetry, with an intermolecular O—O distance of 2.737 Å. The hydrogen bond deviates somewhat from linearity, with an angle between the hydrogen-bonded O—H and the intermolecular O—O line of 8.5° (i.e., the line between the O atom of O(CH₃)₂ and the closer of the two O atoms on H₂O₂). The hydrogen-bonded O—H bond lengthens slightly by 0.02 Å upon complex formation, and the hydrogen bond forms in one of the tetrahedral directions with respect to the proton acceptor oxygen atom. The MP2/6-31+G(d,p) binding energy (ΔE_c) of HOOH:O(CH₃)₂ is -9.6 kcal/mol, while the binding enthalpy at 10 K (ΔH°) is -8.0 kcal/mol.

Discussion

Product Identification. Twin jet co-deposition of samples of Ar/H₂O₂ with samples of Ar/(CH₃)₂O led to product bands at 672 and 1315 cm⁻¹ and a multiplet at 3349 cm⁻¹, with weaker bands observed at 2943, 2829, 1165, 1090, and 914 cm⁻¹ in some experiments. The bands at 672, 1315, and 3349 cm⁻¹ were

observed in all experiments using these same reactants regardless of concentration. In addition, these bands did not change abruptly upon annealing but increased smoothly in approximately the same ratio. These observations suggest that a single product was formed in these experiments. This is consistent with the *ab initio* calculations that found only a single equilibrium structure on the potential surface. The weak bands at 2943, 2829, 1165, 1090, and 914 cm⁻¹ were only observed at low (CH₃)₂O concentration, apparently because they lie very close to parent bands of (CH₃)₂O, and a reduction in the intensity of these parent bands is necessary for the observation of these weak product bands. In the experiments where the bands at 2943, 2829, 1165, 1090, and 914 cm⁻¹ were observed, they appeared to maintain a constant intensity ratio to the primary product bands at 672, 1315, and 3349 cm⁻¹, even after annealing. Thus, the concentration dependence of the product bands also supports formation of a single product species.

With the exception of the bands at 3349 and 672 cm⁻¹, all of the product absorption bands lie near bands observed for either H₂O₂ or (CH₃)₂O. This suggests the formation of a relatively weakly bound molecular complex, in which the two subunits maintain their identities, and are only slightly perturbed by complex formation. This observation is consistent with the *ab initio* calculations which indicate that, with only one exception, the monomer bands are only slightly shifted in the complex. The exception, of course, is the O—H stretching band for the hydrogen-bonded O—H of hydrogen peroxide. This band is shifted dramatically to lower energy and exhibits a significant increase in intensity in the complex relative to the monomer. The red shift of this band and the dramatic increase in its intensity are the infrared spectroscopic signatures of the presence of a hydrogen bond.³² The band centered at 3349 cm⁻¹ has exactly these characteristics and thus confirms the formation of a hydrogen-bonded HOOH:O(CH₃)₂ complex.

Band Assignments. The most intense infrared absorption for the HOOH:O(CH₃)₂ complex is the partially resolved multiplet centered at 3349 cm⁻¹. This band did not shift when (CD₃)₂O was substituted for (CH₃)₂O, indicating that it is a mode associated with the H₂O₂ subunit in the complex, red-shifted by 234 cm⁻¹ relative to H₂O₂. Moreover, this band shifted significantly to 2481 cm⁻¹ when D₂O₂ was substituted for H₂O₂ and had a similar band profile. This further supports the assignment of this band to a vibrational mode of H₂O₂. The ν_H/ν_D ratio for the complex, 3349/2481 = 1.35, indicates hydrogen motion, further supporting the assignment of the band at 3349 cm⁻¹ to the stretching mode of the hydrogen-bonded O—H. These results agree with the MP2/6-31+G(d,p) calculations, which give a computed red shift of 294 cm⁻¹, and a ν_H/ν_D ratio of 1.37.

The bending mode involving the hydrogen-bonded proton is also perturbed in a hydrogen-bonded complex, with a blue-shift often observed.³² The weak product band at 1315 cm⁻¹ is 45 cm⁻¹ higher in energy than the OOH bending mode in HOOH, and this band is assigned to this mode in the 1:1 complex. As expected, the 1315 cm⁻¹ band did not shift with (CD₃)₂O substitution, and it was not present in the D₂O₂ experiments. Because of the low concentration in the D₂O₂ experiment, the OOD bending mode of the complex could not be identified. The *ab initio* calculations place this band in HOOH:O(CH₃)₂ at 1313 cm⁻¹, with a computed blue shift of 20 cm⁻¹ relative to the corresponding band in HOOH, in agreement with the experimental results. The OOD bending mode in DOOD:O(CH₃)₂ is computed to lie at 968 cm⁻¹, blue shifted 15 cm⁻¹ from the bending mode in D₂O₂.

TABLE 2: Observed and Computed Band Positions for the $\text{H}_2\text{O}_2 \cdot \text{O}(\text{CH}_3)_2$ Complex

computed			experimental			
parent	complex	shift	parent	complex	shift	description
	790		672			hydrogen bond libration
956	941	-15	925	914	-11	COC symmetric stretch
1140	1131	-9	1098	1090	-8	COC antisymmetric stretch
1182	1186	+4	1168	1165	-3	CH_3 rock
1293	1313	+20	1270	1315	+45	antisymmetric HOOH bend
3069	3093	+27	2820	2826	+6	antisymmetric CH_3 stretch
3142	3178	+36	2889	2987	+8	symmetric CH_3 stretch
3148	3185	+37	2922	2943	+21	antisymmetric CH_3 stretch
3242	3253	+11	2986	2997	+11	antisymmetric CH_3 stretch
3823	3530	-293	3583	3349	-234	hydrogen bonded O-H stretch

The weak product bands at 2943, 2829, 1165, 1090, and 914 cm^{-1} fall within 10–20 cm^{-1} of parent modes of $(\text{CH}_3)_2\text{O}$. These bands are assigned on the basis of their proximity to the unperturbed ether subunit bands, as shown in Table 1, and by comparison to the MP2/6-31+G(d,p) calculations. A comparison of the experimental and computed vibrational frequencies is presented in Table 2. In general, both the magnitude and direction of the experimental shifts are modeled very well by the calculations. As will be discussed below, the direction and magnitude of the shifts of these modes are similar to those observed for other hydrogen-bonded complexes of $(\text{CH}_3)_2\text{O}$. The ether subunit product bands seen in the experiments with $(\text{CD}_3)_2\text{O}$ were identified in a similar manner and are also listed in Table 1.

The formation of a 1:1 complex results in the loss of three translational and three rotational degrees of freedom and the creation of six new intermolecular vibrational modes. For a weakly bound complex, these new intermolecular modes typically lie at very low frequencies. The product band at 672 cm^{-1} has a relatively high energy, but it does not lie near any vibrational mode of either subunit in the complex. There are two intermolecular vibrational modes in which the hydrogen-bonded H atom moves away from the hydrogen-bonding O–O axis. The computed frequency of the higher energy mode of this type is 790 cm^{-1} . All other modes have computed frequencies that lie below the spectral range of the spectrometer used in this study. It was observed experimentally that the 672 cm^{-1} band did not shift upon deuteration of the $(\text{CH}_3)_2\text{O}$ subunit, in agreement with the calculations. Thus, the 672 cm^{-1} band is assigned to an intermolecular mode of the complex. The motion of the hydrogen-bonded proton in this mode distorts the hydrogen bond further from linearly and thus occurs at a much higher frequency than the other intermolecular modes. For comparison, the highest frequency for an intermolecular mode in the more strongly bound $\text{FH}:\text{O}(\text{CH}_3)_2$ complex has been reported at 801 cm^{-1} . For the $\text{DOOD}:\text{O}(\text{CH}_3)_2$ complex, a very weak band was observed at 501 cm^{-1} and has been tentatively assigned as the deuterium counterpart of the 672 cm^{-1} band. Since this vibration mainly involves the motion of the deuterium that is hydrogen-bonded, the harmonic ratio $\nu_{\text{H}}/\nu_{\text{D}}$ should be about 1.4. The ratio of 672/501 gives a value of 1.34. The ab initio calculations place this mode at 570 cm^{-1} for the $\text{DOOD}:\text{O}(\text{CH}_3)_2$ complex, with a ratio 790/570 = 1.39.

Alternatively, assignment of the 672 cm^{-1} band to the nearest intramolecular mode might be considered, namely, the O–O stretching mode of H_2O_2 . However, this mode is observed experimentally near 900 cm^{-1} , which would require a shift of more than 200 cm^{-1} upon complex formation, or a $\Delta\nu/\nu$ of nearly 25%. For comparison, the O–H stretch of the hydrogen-bonded hydrogen, which is the most sensitive mode to complexation, was only observed to shift 7%. In addition, this mode

TABLE 3: Frequency Shifts for Selected $(\text{CH}_3)_2\text{O}$ Complexes

Lewis acid	$\Delta\nu_s$ (cm^{-1})	$\Delta\nu_s/\nu_s$
H_2O^a	131	0.036
H_2O_2	234	0.065
HCl^b	552	0.193
HF^c	569	0.145

^a From ref 13. ^b From ref 15. ^c From ref 14.

is calculated to lie more than 200 cm^{-1} to higher energy than is observed experimentally and to shift only 2 cm^{-1} upon complex formation. Finally, this mode is computed to have a small (7 cm^{-1}) deuterium shift, whereas a large (672–501 = 171 cm^{-1}) shift was observed. Thus, assignment to the O–O stretching mode is not realistic and assignment to the intermolecular mode described above is made.

While additional vibrational modes of both subunits in the complex are anticipated, these modes were all calculated to fall less than 1 cm^{-1} away from the corresponding parent band (i.e., not very sensitive to complex formation) and were thus not observable underneath the intensity of the parent bands.

Further Comparisons. The study reported here of the hydrogen-bonded $\text{HOOH}:\text{O}(\text{CH}_3)_2$ complex represents the first definitive identification of a hydrogen-bonded complex of solvent-free H_2O_2 . As such, it is of interest to compare spectral features of this complex to complexes of other proton donors to the same base. In 1983, Barnes and Beech reported¹³ the characterization of the analogous complex that has H_2O as the proton donor, $\text{HOH}:\text{O}(\text{CH}_3)_2$. In this complex, the hydrogen-bonded proton stretching mode red-shifted 131 cm^{-1} relative to H_2O , which is a smaller shift than that observed for $\text{HOOH}:\text{O}(\text{CH}_3)_2$, as shown in Table 3. Since these complexes are structurally similar, the larger shift for $\text{HOOH}:\text{O}(\text{CH}_3)_2$ indicates that H_2O_2 is a stronger proton donor than H_2O for hydrogen bonding. On the other hand, the shift in $\text{HOOH}:\text{O}(\text{CH}_3)_2$ is significantly less than that observed for the corresponding complexes having HF and HCl as proton donors,^{14,15} indicating that HF and HCl are stronger proton donors than H_2O_2 . These observations are consistent with the computed MP2/6-31+G(d,p) binding energies of these complexes, which indicate that $\text{HOOH}:\text{O}(\text{CH}_3)_2$, with an electronic binding energy (ΔE_e) of -9.6 kcal/mol, is more stable than $\text{HOH}:\text{O}(\text{CH}_3)_2$ ($\Delta E_e = -7.3$ kcal/mol) but less stable than $\text{FH}:\text{O}(\text{CH}_3)_2$ ($\Delta E_e = -11.9$ kcal/mol).

Acknowledgment. The authors gratefully acknowledge support of this research by the National Science Foundation, through grant CHE 98-77076.

References and Notes

- (1) Gregoire, P. J.; Chaumerliac, N.; Nickerson, E. C. *J. Atmos. Chem.* **1994**, *18*, 247.
- (2) Sakugawa, H.; Kaplan, I. R. The Chemistry of Atmospheric Hydrogen Peroxide in Southern California. In *Gaseous Pollutants*; Nriagu, J. O., Ed.; John Wiley and Sons: New York, 1992; Vol. 24.
- (3) *Oxidative Stress, Cell Activation and Viral Infection*; Pasquier, C., Ed.; Birkhauser Verlag: Basel, Boston, 1994; p 358.
- (4) Benassi, R.; Fiandri, L. G.; Taddei, F. *J. Org. Chem.* **1995**, *60*, 5855.
- (5) Bach, R. D.; Su, M.-D.; Schlegel, H. B. *J. Am. Chem. Soc.* **1994**, *116*, 5379.
- (6) Bach, R. D.; Owensby, A. L.; Gonzalez, C.; Schlegel, H. B.; McDouall, J. J. W. *J. Am. Chem. Soc.* **1991**, *113*, 6001.
- (7) Cradock, S.; Hinchcliffe, A. *Matrix Isolation*; Cambridge University Press: Cambridge, U.K., 1975.
- (8) Whittle, E.; Dows, D. A.; Pimentel, G. C. *J. Chem. Phys.* **1954**, *22*, 1943.
- (9) Lannon, J. A.; Verderame, F. D.; Anderson, R. W. *J. Chem. Phys.* **1971**, *54*, 2212.

- (10) Tso, T.-L.; Lee, K. C. *J. Phys. Chem.* **1985**, *89*, 1612.
- (11) Catalano, E.; Sanborn, E. *J. Chem. Phys.* **1963**, *38*, 2273.
- (12) Petterson, M.; Tuominen, S.; Rasanen, M. *J. Phys. Chem.* **1997**, *101*, 1166.
- (13) Barnes, A. J.; Beech, T. R. *Chem. Phys. Lett.* **1983**, *94*, 568.
- (14) Andrews, L.; Johnson, G. L.; Davis, S. R. *J. Phys. Chem.* **1985**, *89*, 9, 1710.
- (15) Schriver, L.; Loutellier, A.; Burneau, A.; Perchard, J. P. *J. Mol. Struct.* **1982**, *95*, 37.
- (16) Lu, C.-S.; Hughes, E. W.; Giguere, P. A. *J. Am. Chem. Soc.* **1941**, *63*, 1507.
- (17) Ault, B. S. *J. Am. Chem. Soc.* **1978**, *100*, 2426.
- (18) Pople, J. A.; Binkley, J. S.; Seeger, R. *Int. J. Quantum Chem. Quantum Chem. Symp.* **1976**, *10*, 1.
- (19) Krishnan, R.; Pople, J. A. *Int. J. Quantum Chem.* **1978**, *14*, 91.
- (20) Bartlett, R. J.; Silver, D. M. *J. Chem. Phys.* **1975**, *62*, 3258.
- (21) Bartlett, R. J.; Purvis, G. D. *Int. J. Quantum Chem.* **1978**, *14*, 561.
- (22) Hehre, W. J.; Ditchfield, R.; Pople, J. A. *J. Chem. Phys.* **1972**, *56*, 2257.
- (23) Hariharan, P. C.; Pople, J. A. *Theor. Chim. Acta* **1973**, *28*, 213.
- (24) Spitznagel, G. W.; Clark, T.; Chandrasekhar, J.; Schleyer, P. v. R. *J. Comput. Chem.* **1983**, *3*, 3633.
- (25) Clark, T.; Chandrasekhar, J.; Spitznagel, G. W.; Schleyer, P. v. R. *J. Comput. Chem.* **1983**, *4*, 294.
- (26) Del Bene, J. E.; Person, W. B.; Szczepaniak, K. *J. Phys. Chem.* **1995**, *99*, 10705.
- (27) Del Bene, J. E.; Shavitt, I. In *Molecular Interactions: From van der Waals to Strong Bound Complexes*; Scheiner, S., Ed.; John Wiley and Sons: Chichester, U.K., 1997; pp 157–179.
- (28) Del Bene, J. E. In *The Encyclopedia of Computational Chemistry*, Schleyer, P. v.R., Allinger, N. L., Clark, T., Gasteiger, J., Kollman, P. A., Schaefer, H. F., III, Scheiner, P. R., Eds.; John Wiley and Sons: Chichester, U.K., 1998; Vol. 2, pp 1263–1271.
- (29) Del Bene, J. E.; Jordan, M. J. T. *Int. Rev. Phys. Chem.* **1999**, *18*, 119.
- (30) Frisch, M. J.; Trucks, G. W.; Schlegel, H. B.; Gill, P. M. W.; Johnson, B. G.; Robb, M. A.; Cheeseman, J. R.; Keith, T.; Petersson, G. A.; Montgomery, J. A.; Raghavachari, K.; Al-Laham, M. A.; Zakrzewski, V. G.; Ortiz, J. V.; Foresman, J. B.; Cioslowski, J.; Stefanov, B. B.; Nanayakkara, M.; Challacombe, M.; Peng, C. Y.; Ayala, P. Y.; Chen, W.; Wong, M. W.; Andres, J. L.; Binkley, J. S.; Defrees, D. J.; Baker, J.; Stewart, J. P.; Head-Gordon, M.; Gonzalez, C.; Pople, J. A. *Gaussian 94*; Gaussian, Inc.: Pittsburgh, PA, 1995.
- (31) Lassegues, J.-C.; Grenie, Y.; Forel, M.-T. *Compt. Rend. Acad. Sci. Paris* **1970**, *B271*, 421.
- (32) Pimentel, G. C.; McClellan, A. L. *The Hydrogen Bond*; W. H. Freeman: San Francisco, 1960.